Detailed Performance Assessment of 16% Blockage Interrupted Ribs at 60^o Inclination in a Square Section Turbine Blade Cooling Passage

C.L.P. Tsang, D.R.H. Gillespie, P.T. Ireland
Department of Engineering Science
University of Oxford
Parks Road
Oxford, OX1 2PJ
United Kingdom

G.M. Dailey
Turbine Aerothermal
Rolls-Royce Plc.
Moor Lane, Derby, DE24 8BJ
United Kingdom

Abstract

Three conventional configurations of 60^{o1} inclined, interrupted ribs at 16% blockage[2] were tested using a large-scale model of a cooling passage inside a turbine blade. Transient heat transfer experiments using liquid crystal were used to determine the full distribution of local heat transfer coefficient. Heat transfer data on all gas swept surfaces, including heat transfer level on the roughness elements themselves were obtained and compared with data in the literature. The passage thermal efficiency is also presented using pressure loss measurements. Finally detailed flow field at the end of the ribbed section were measured using a miniature 4-hole pyramid probe and the data are used to interpret the heat transfer results.

Introduction

The advantages of using ribs in turbine blade cooling passages have been known for many years and are well understood. However, almost all results and conclusions are from investigations based on ribs that have blockage ratio less than 10% such as Han et al. (1991), Kukreja et al. (1992), Wang et al. (1996) and Rau et al. (1998). It is also known that large roughness elements introduce a disproportionately high pressure loss. Nevertheless, turbine blade casting limitations restrict the minimum size of a roughness element that can be manufactured in an internal cooling passage, to the extent that the blockage ratio of the roughness elements can be large, especially in turbine blades of a small engine. It is also likely that the experimental correlations obtained for low blockage ribs may not be applicable to high blockage ribs. There are very little data in the literature for high blockage (15% e/d or above) turbulators, though the group at the Northeastern University, Taslim et al. (1996) have produced some useful data. The lack of data for high blockage ratio ribs in the literature is the main driving force for the research presented here. The current investigation included heat transfer and pressure measurements of three conventional configurations at 16% blockage in a square cross section passage.

The performance of a particular configuration can be evaluated using the following two parameters,

Heat transfer enhancement factor, defined as $EF = Nu/Nu_s$
Thermal efficiency, defined as $Eff = (Nu/Nu_s)/(f/f_s)$

[1] Measured from the stream-wise direction
[2] Defined as turbulator height divided by passage hydraulic diameter

Paper presented at the RTO AVT Symposium on "Advanced Flow Management: Part B – Heat Transfer and Cooling in Propulsion and Power Systems", held in Loen, Norway, 7-11 May 2001, and published in RTO-MP-069(I).

Report Documentation Page

Form Approved
OMB No. 0704-0188

Public reporting burden for the collection of information is estimated to average 1 hour per response, including the time for reviewing instructions, searching existing data sources, gathering and maintaining the data needed, and completing and reviewing the collection of information. Send comments regarding this burden estimate or any other aspect of this collection of information, including suggestions for reducing this burden, to Washington Headquarters Services, Directorate for Information Operations and Reports, 1215 Jefferson Davis Highway, Suite 1204, Arlington VA 22202-4302. Respondents should be aware that notwithstanding any other provision of law, no person shall be subject to a penalty for failing to comply with a collection of information if it does not display a currently valid OMB control number.

1. REPORT DATE	2. REPORT TYPE	3. DATES COVERED
00 MAR 2003	**N/A**	**-**

4. TITLE AND SUBTITLE	5a. CONTRACT NUMBER
Detailed Performance Assessment of 16% Blockage Interrupted Ribs at Sixty Degree Inclination in a Square Section Turbine Blade Cooling Passage	5b. GRANT NUMBER
	5c. PROGRAM ELEMENT NUMBER
6. AUTHOR(S)	5d. PROJECT NUMBER
	5e. TASK NUMBER
	5f. WORK UNIT NUMBER
7. PERFORMING ORGANIZATION NAME(S) AND ADDRESS(ES) **NATO Research and Technology Organisation BP 25, 7 Rue Ancelle, F-92201 Neuilly-Sue-Seine Cedex, France**	8. PERFORMING ORGANIZATION REPORT NUMBER
9. SPONSORING/MONITORING AGENCY NAME(S) AND ADDRESS(ES)	10. SPONSOR/MONITOR'S ACRONYM(S)
	11. SPONSOR/MONITOR'S REPORT NUMBER(S)

12. DISTRIBUTION/AVAILABILITY STATEMENT
Approved for public release, distribution unlimited

13. SUPPLEMENTARY NOTES
Also see ADM001490, presented at RTO Applied Vehicle Technology Panel (AVT) Symposium held in Leon, Norway on 7-11 May 2001, The original document contains color images.

14. ABSTRACT

15. SUBJECT TERMS

16. SECURITY CLASSIFICATION OF:			17. LIMITATION OF ABSTRACT	18. NUMBER OF PAGES	19a. NAME OF RESPONSIBLE PERSON
a. REPORT	b. ABSTRACT	c. THIS PAGE			
unclassified	**unclassified**	**unclassified**	**UU**	**14**	

where subscript, s is for the all-smooth walls values. Normally the optimization problem can be thought of as equivalent to selecting the system that achieves a particular Nusselt number enhancement with the lowest friction factor. In small blockage systems, an increase in blockage ratio generally results in an increase in heat transfer enhancement as well as a higher pressure loss with the associated requirement for higher pumping power.

Experimental apparatus

A drawing of the experimental apparatus is shown in Figure 1. It consists of a square cross-section (50mm x 50mm internal dimension) passage that is 3000mm long. The passage is made of clear perspex, 12mm thick to provide optical access to the temperature sensitive liquid crystals applied to the inner surface. The large-scale enables engine Reynolds numbers to be achieved at low speed and at near atmospheric pressure. Experiments have been performed over a range of Reynolds numbers from 20,000 to 60,000 which is representative of typical engine values. The air is heated just inside the tunnel inlet by a uniform heater mesh, Gillespie (1996). The mesh time constant in the present experiments was calculated to be insignificant compared to the time for the liquid crystal coated perspex surface to change colour. Air is drawn through the duct and through an orifice plate flow meter by a suction pump. Heating of the perspex duct wall commences when the mesh current supply is switched on. The ribbed test sections were placed 2 metres (20d) downstream of inlet. Tsang et al (2000) showed that a steady, developed flow was established ahead of the ribbed section. Two inclined mirrors were placed above and below the test section to provide optical access for three surfaces from a single camera position. Note that rib geometry symmetry meant that there was no need to measure htc on both ribbed surfaces. For the configuration with only one ribbed wall, two tests were required to obtain htc on all surfaces from one camera view.

The configurations tested were shown in Table 1.

Configuration	Blockage Ratio (%)	Facing Wall Ribs Alignment
A	16	In-line, parallel
B	16	Crossed
C	16	One rib wall only
D	0	N/A

Table 1 List of the configurations tested, graphical representations of each configuration are shown in figure 2.

All the configurations were tested with a rib pitch length of 8 times the height of the turbulators. This pitch value was chosen from data in the literature, Taslim and Spring (1995) which showed e/d of around 8 gave the best result. Ribs were positioned inline on opposite walls for the parallel rib configuration. For the crossed ribs system, ribs were inclined with opposing angles on two facing walls.

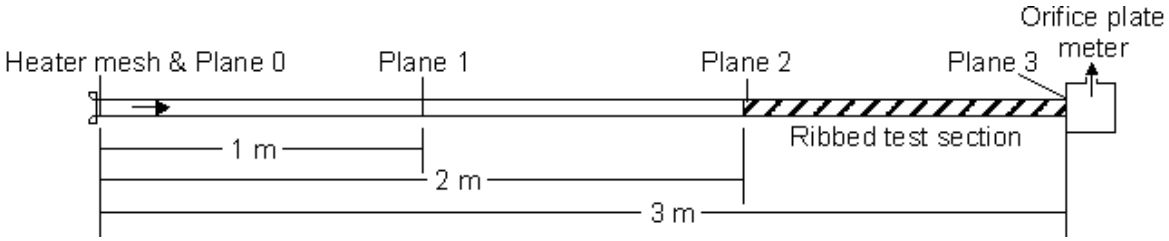

Figure 1 Drawing of the test facility

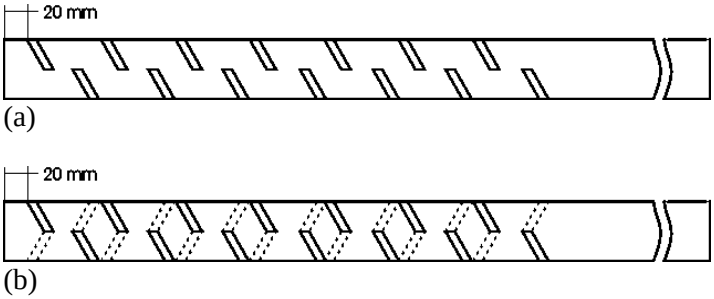

Figure 2 Illustration of the test configurations. (a) 16% e/d, 60^o in-line. (b) 16% e/d, 60^o cross, dotted lines represent the rib positions on the facing wall.

Turbulators details

All the turbulators used had a square cross-section with external dimensions of 8mm, which corresponded to 16% blockage ratio. The turbulators were cut from hollow copper square shaped tube and with their ends were sealed. It is important to have a low Biot number material in order to maintain uniform temperature across ribs. The rib data reduction technique for the rib htc was described in Wang et al. (1996). The edges of the turbulators are rounded with 1mm radius.

Pressure measurement

The average friction loss were determined from static pressure measurements in a section of developed flow. 17 static pressure tapping were located on the top wall of the test section and another 5 on the bottom wall. Note that the passage was orientated so that the ribs were positioned on the sidewalls and the top and bottom walls were smooth. The location of these pressure tapping is indicated in Figure 3.

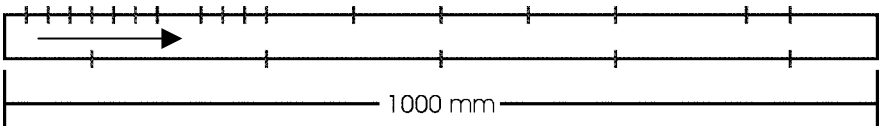

Figure 3 Locations of the static pressure measurement

The friction factor was related to the pressure gradient under developed flow conditions by

$$f = \frac{1}{0.5\rho U^2}\frac{d}{4}\frac{dP}{dx} \qquad \textbf{Eqn. 1}$$

The measured friction factor for the smooth wall passage was within 7% of the correlation given by Blasius,

$$f_s = 0.079 \times Re^{-0.25} \qquad \textbf{Eqn. 2}$$

Figure 4 shows the variation of pressure difference through the test section for the 60^o inline, parallel rib configuration. Despite the large initial fluctuations where measurements were close to the turbulators at the start of the section, the pressure gradient reaches a fairly constant level after 6d. The average friction factor were evaluated from the developed region of each configuration, which was chosen to be between the 3rd row and 7th row ribs. The best-fit lines are shown in the figure.

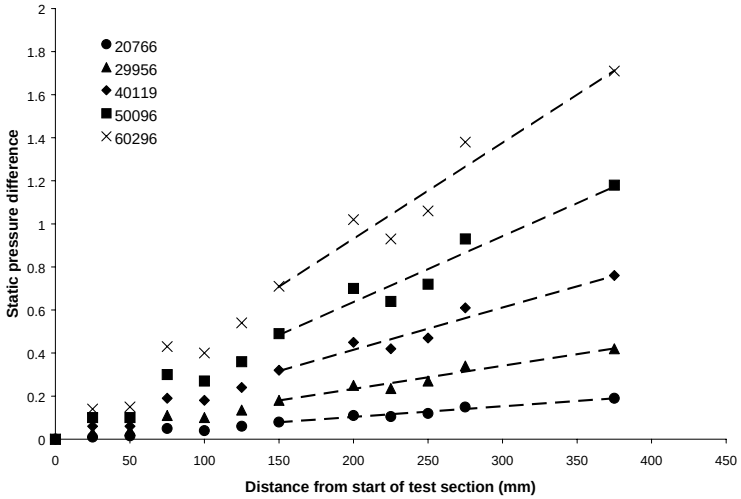

Figure 4 Static pressure difference from the start of the section for 16% 60^o in-line, parallel configuration at different Reynolds numbers.

Temperature measurements

The gas temperatures were measured at four planes along the passage. The first was immediately behind the heater mesh, and the others were positioned 1, 2 and 3m downstream of the mesh. At each of these planes, nine fast response thermocouples were mounted on a nylon mesh to measure gas temperature, Ireland et al. (2001). The temperature history of each thermocouple was logged throughout the tests using a data acquisition system.

Heat transfer data were obtained using single narrow-band thermochromic liquid crystals applied to the inner surface of the passage. Surface thermocouples were glued to the inner surface to calibrate the liquid crystal. The difference between the htc calculated from the thermocouple signal and the liquid crystal was found to be less than 5%. The average temperature over the turbulators was deduced from processing the intensity change of the liquid crystal underneath. Thermocouples were also embedded in one rib for each configuration to check the rib htc calculated from the liquid crystal analysis. For the analysis of the turbulator average htc, see Wang et al. (1996).

The intensity change of the liquid crystal coating was captured by a video camera during the experiments and the images were then digitised using a PC frame grabber after the experiment. The heat transfer coefficients were calculated from the surface temperature response under convective heating, set out in Eqn. 3, Carslaw and Jaeger (1959) together with the use of the superposition theorem, Eqn. 4 and 5, Metzger and Larson (1986), to account for the change of driving gas temperature during the experiments.

$$T_{w1} = T_{w0} + \left(T_f - T_{w0}\right)\left[1 - \exp\left(\frac{h^2 t}{\rho c k}\right) erfc\left(\frac{h\sqrt{t}}{\sqrt{\rho c k}}\right)\right] \qquad \textbf{Eqn. 3}$$

$$T - T_i = \sum_1^n U\left(t - t_i\right)\Delta T_m \qquad \textbf{Eqn. 4}$$

where $$U\left(t - t_i\right) = 1 - \exp\left[\frac{h^2\left(t - t_i\right)}{\rho c k}\right] erfc\left[\frac{h\sqrt{\left(t - t_i\right)}}{\sqrt{\rho c k}}\right] \qquad \textbf{Eqn. 5}$$

Flow measurement

A miniature 4 hole pyramid probe was used to measure the flow field inside the passage. The probe geometry is similar to that used previously at Oxford, Main et al. (1996). The relationship between yaw, pitch and total pressure coefficient was determined from a careful calibration exercise. The outside diameter of the probe is 1.3mm so that the probe blockage was less than 0.06% and it was mounted on a stepper motor driven traverse system to measure the flow field across a plane positioned six rib heights downstream of the last rib.

Pressure Loss Results

Friction factors were normalized using the data from the 16% 60^o configuration and the comparison of friction factors to the closest data from the literature is shown in Figure 5. It can be seen that the friction factors of the configurations compared change very little with Reynolds numbers, and the configurations tested in the current study have significantly smaller friction factor than the transverse ribs reported previously. At the same blockage (16%), the friction factor of the transverse rib configuration is one and a half times the friction factor of the inclined, interrupted ribs tested and the 45^o continuous ribs configuration has higher friction factor than all the 60^o broken ribs configuration tested. This shows that a large reduction in pressure loss can be achieved if ribs are placed at an angle to the mainstream flow in an interrupted configuration. Another interesting observation from the figure is that the single 16% blockage ribbed wall configuration has a lower pressure drop than the 6.25% e/d, 45^o ribs configuration despite the larger overall blockage.

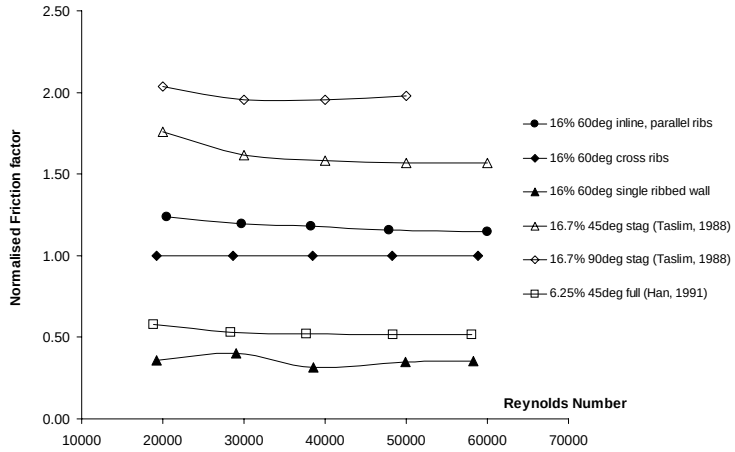

Figure 5 Normalised average friction factors for all configurations at various Reynolds numbers

Heat Transfer Results

Heat transfer data obtained from the current study are based on the local mixed bulk temperature. The htcs were first calculated using the average temperature of the nine thermocouples on the plane just upstream of the test section (2m downstream from inlet). This average temperature was shown, see Ireland et al. (2001), to give a good measure of the mixed bulk temperature after an investigation on the velocity and temperature profile was conducted. With the full surface htc data, h based on local mixed bulk temperature can be deduced from the htc data based on an upstream temperature using the energy balance method proposed by Metzger et al. (1986). This method was considered in the light of detailed gas temperature measurements by Tsang et al. (2000). They presented Eqn. 6 relating htc based on mixed bulk temperature to h based on the entry mixed bulk temperature. The extra parameter, Ψ accounts for the non-isothermal wall

temperature in a transient heat transfer test, Tsang et al. (2000) and was shown to be approximately unity.

$$\frac{h_{mb}}{h_E} = \frac{1}{1 - \psi \frac{\int_A h_E dA}{mc_p}} \qquad \textbf{Eqn. 6}$$

A smooth walled passage was tested first to commission the test facility and to establish base line enhanced data. The htc distribution of the smooth walled passage is shown in Figure 6 and has been reported in Tsang et al. (2000). The average htc calculated was found to be 10% below the htc of the fully developed value from Dittus-Boelter. The difference in the flow field between pipe flow and square passage flow is thought to explain the different heat transfer level between the empirical data obtained in the facility and the Dittus-Boelter equation.

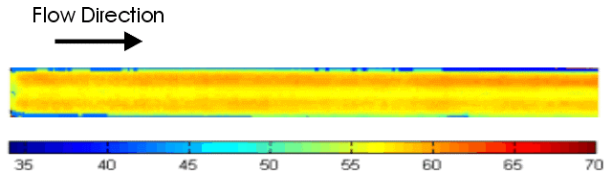

Figure 6 Smooth Wall htc distribtion at Re 50,000

The detailed local htc distributions for each configuration at a Reynolds number of 50000 are shown in Figure 7 to Figure 9. All surfaces: top wall, ribbed wall, bottom wall and smooth wall (in the case of configuration C) are included in each figure. The red lines and letters illustrate the common edges for the sets of surfaces. The numbers at the rib locations represent the overall htc of the rib based on the rib footprint area. It can be seen that a periodic pattern was established on the surface between ribs after 3 rows of ribs for all configurations. The heat transfer results presented below are value averaged between the 4th and 7th rib row. Because of the different secondary flow structure in each configuration, different pattern of htc results can be seen. There are several common features that can be extracted from these figures.

1) Low htc region behind the upper ribs caused by the flow separation over the ribs top.
2) There is virtually no flow separation downstream of the lower ribs. The flow is more aligned with the lower rib axis than for the upper ribs due to the secondary flow.
3) High htc behind the trailing edge of the upper ribs due to the turbulence induced by the flow separation.

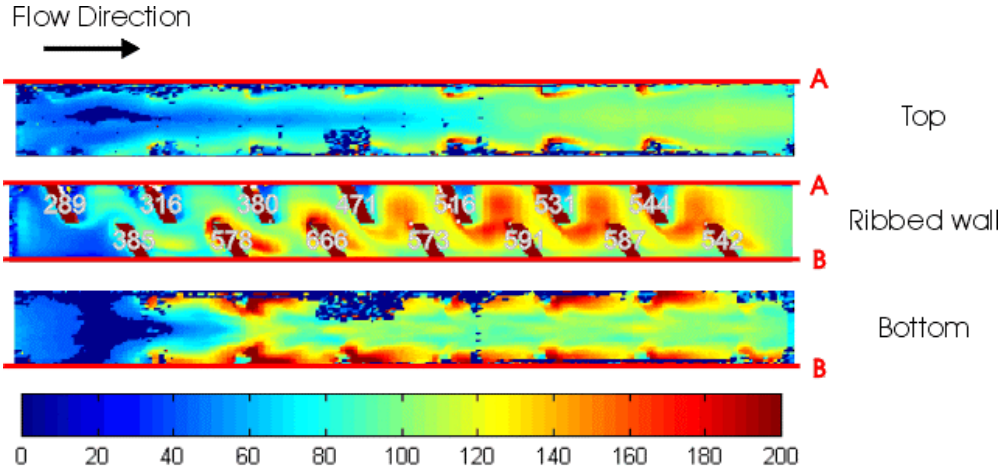

Figure 7 Htc distribution for configuration A at Re 50,000

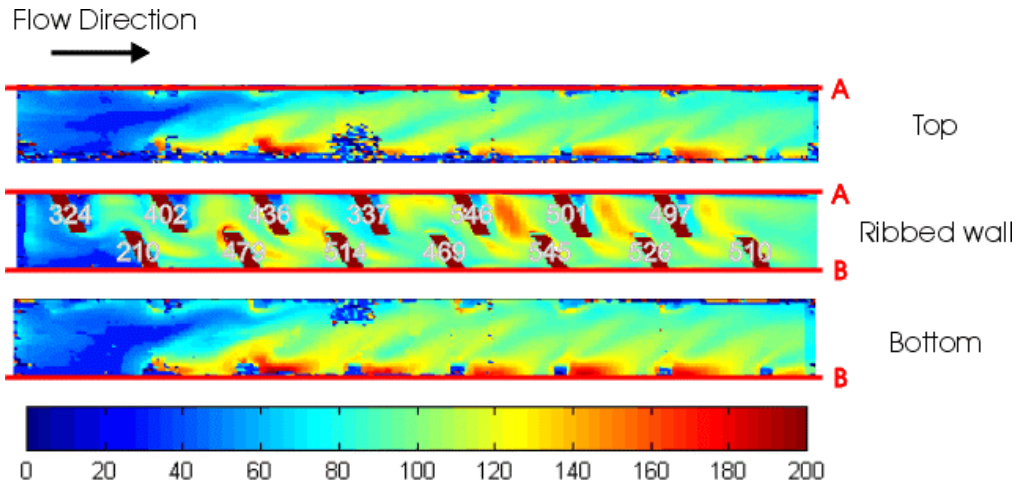

Figure 8 Htc distribution for configuration B at Re 50,000

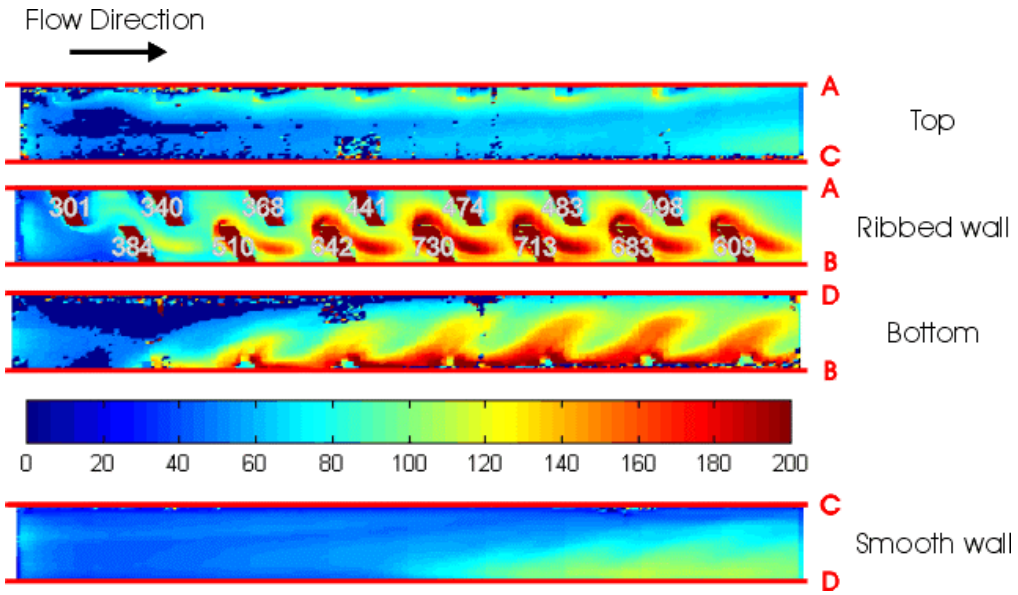

Figure 9 Htc distribution for configuration C at Re 50,000

The flow measurements using the miniature 4 hole pyramid probe at a plane 6e (where e = rib height) downstream of the last ribs are illustrated in Figure 10.

Two counter rotating vortices can be observed in the parallel rib configuration, Figure 10 (a). A similar observation was reported by Fann et al. (1994) in lower rib blockage systems. These counter-rotating vortices bring the core flow to the wall, and this improves flow mixing and results in the high averaged htc of this configuration reported later in this paper. On the other hand, both the crossed ribs and the single ribbed wall configurations induce a single vortex inside the passage. There is a significant velocity gradient in the profile for these two configuration, the core flow is traveling at high velocity, with little flow mixing in the ribbed section, and this results in a lower htc than the parallel rib configuration.

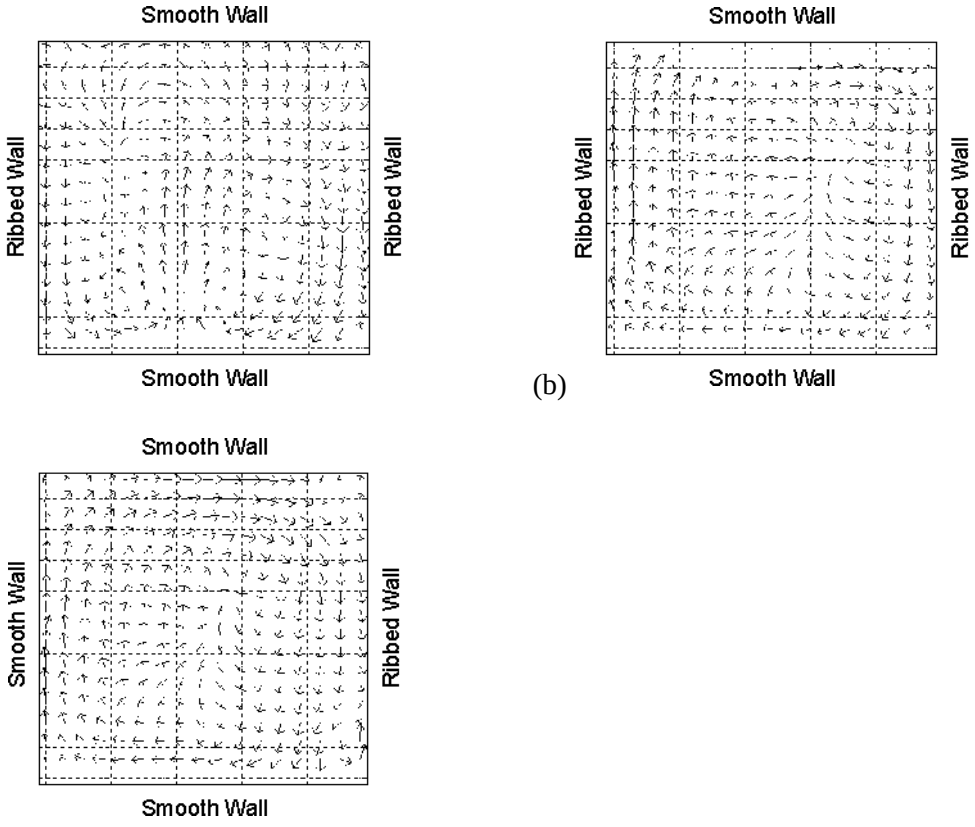

Figure 10 Flow field visualization of the 16% 60^0, (a) in-line, parallel ribs, (b) crossed ribs and (c) single ribbed wall configuration at Re 56,000

The variation of the effective htc on the ribs with Reynolds number is shown in Figure 11. For all the configurations, it can be seen that ribs located on the lower half of the passage have higher htc than those on the upper half. Apart from the upper ribs for the in-line, parallel configuration which continue to increase, all other ribs reach a fairly flat heat transfer level after 4 rows. The turbulators in the in-line, parallel rib configuration have similar htc toward the end of the ribbed section, together with an even htc distribution on the surface between ribs as shown in Figure 7, this configuration gives a more evenly distributed htc pattern in the developed region. It can be seen that the most upstream ribs (first row, upper ribs) have similar htc in all configurations at similar Reynolds number, but the second most upstream ribs (first row, lower ribs) in the parallel configuration has much higher htc than the same ribs in another two configurations, this demonstrates that the inclination of the first ribs has started to change the flow direction if two inclined ribs are positioned in-lined on two opposite walls. The upper rib level in the single ribbed wall configuration changes very little along the ribbed section, and this shows that no significant benefit is obtained from the secondary flow as in the other two configurations.

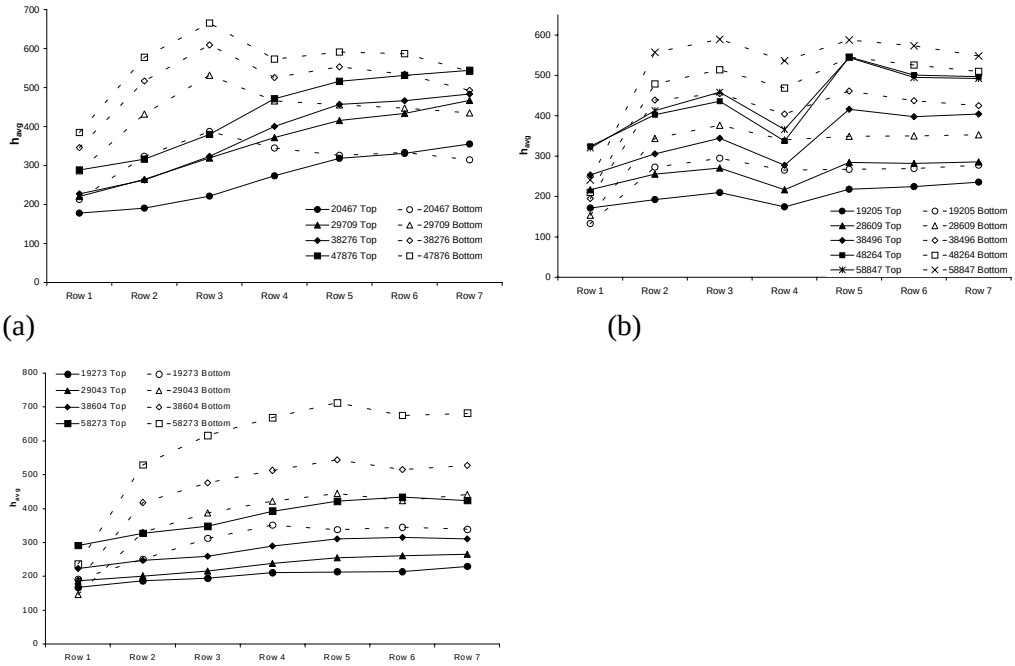

(a) (b)

(c)

Figure 11 Effective ribs htc of 16% 60^o, (a) in-line, parallel (b) cross and (c) single ribbed wall, configurations at different Reynolds numbers

For clearer results comparison, the heat transfer results presented below were normalized from the 16% 60^o cross rib configuration data. The normalised, average htc levels in the developed region on the ribbed wall are compared in Figure 12. Data for the lower blockage ribs, Han et al. (1991) and configurations with similar blockage, but different ribs incidence, Taslim and Spring (1988) are also included. Han's data include the contribution from the ribs. However, Taslim's data are the htc data on the surface between ribs only, no information was given on the ribs themselves, hence the average heat transfer level should be larger than compared here. It can be seen that transverse ribs should have the highest htc level if heat transfer on the ribs is included. The single ribbed wall configuration yields the lowest htc level in the comparison. The in-line, parallel rib configuration is the only geometry tested that has a higher htc level than the 6.25% configuration. Although the bigger turbulators induce stronger secondary vortices, hence better flow mixing, as the ribs pitch stays roughly the same, the smaller blockage systems benefits from the smaller flow separation over the ribs top. The in-line, parallel rib configuration produces the highest heat transfer enhancement of the configurations tested. The crossed rib configuration gives lower heat transfer enhancement due to the lack of flow mixing, Figure 10 (b). Flow measurements showed that the single ribbed wall and the crossed rib appear to induce a similar strength single vortex. The flow measurement was carried out at a plane downstream of the last ribs, and htc level reported here are the averaged values between rib rows 4 and row 7. The htc distribution on the smooth wall in Figure 9 showed that this strong vortex has yet to establish, this could explain the difference in the htc level between these two configurations.

Generally, the heat transfer enhancement decreases with an increase in Reynolds number. This could mean the effect of the secondary flow induced by turbulators become less significant as the axial velocity of the main stream flow increases, in particular, at the high Reynolds number tested, there is little difference in the heat transfer enhancement achieved by different configurations.

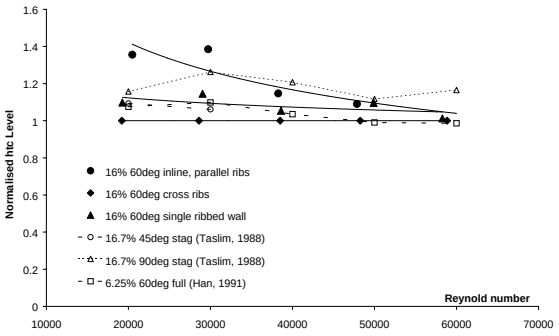

Figure 12 Normalised heat transfer level on the ribbed wall

It is often desirable to cool the pressure and suction sides of the passage without excessive cooling of the web regions in order to minimise thermal stresses, and hence increase blade life. The introduction of turbulators in internal passages not only gives heat transfer enhancement on the ribbed walls, but also on the adjacent smooth walls due to the secondary flow induced. For this reason, it is important for the blade designer to have information about the htc level on the smooth walls as well as the ribbed wall. Figure 13 shows a compilation of the normalised average htc level on the top passage wall. Figure 14 shows the summary of the normalised average htc level on the bottom passage wall. The heat transfer level is much higher than the smooth wall value, especially on the bottom passage wall in all the configurations tested. The single vortex secondary flow system in the crossed ribs configuration gives similar heat transfer on top and bottom walls, at the same time, heat transfer on the top wall is much higher than the bottom wall in the parallel ribs and single ribbed wall configurations. There is little effect the single ribbed wall configuration has on the top passage wall, as the vortex seen in Figure 10(c) has not been established.

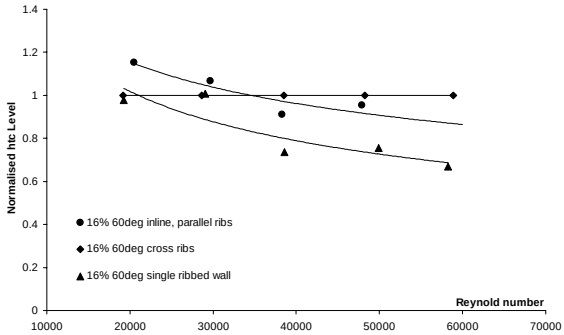

Figure 13 Summary of normalised average htc level on top passage wall

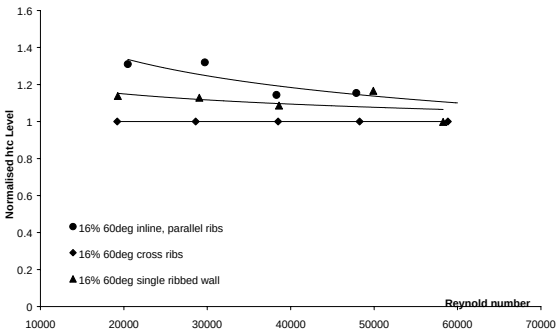

Figure 14 Summary of normalised average htc level on bottom passage wall

The normalised overall htc level over the developed region for each configuration tested is shown in Figure 15. The heat transfer enhancement over the whole test section was compared to the results calculated from convective efficiency using isothermal wall analysis, Ireland et al. (2001). Results from the current study were within 6% of the results from the convective efficiency analysis. This confirms agreement between the experimental technique using liquid crystals and the energy balance approach.

The normalized thermal efficiency of the ribbed wall of all geometries is compared in Figure 16. The best and the least efficient configuration are 16% e/d, 60^o single ribbed wall configuration and 16%e/d, staggered, transverse rib respectively. The former configuration achieves good thermal efficiency by having a reasonably high htc on the ribbed wall and maintaining a very small pressure loss at the same time. Although the latter achieved the highest heat transfer in the current study, the penalty of the large profile drag on the traverse ribs brings the thermal efficiency down.

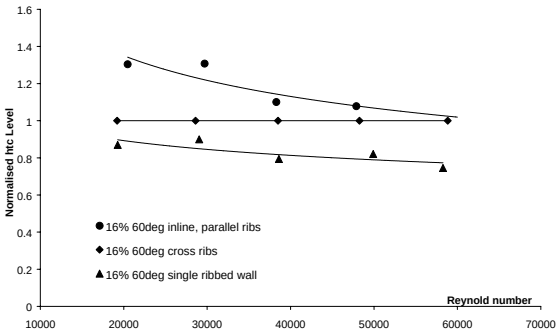

Figure 15 Summary of normalised overall htc level across the developed region

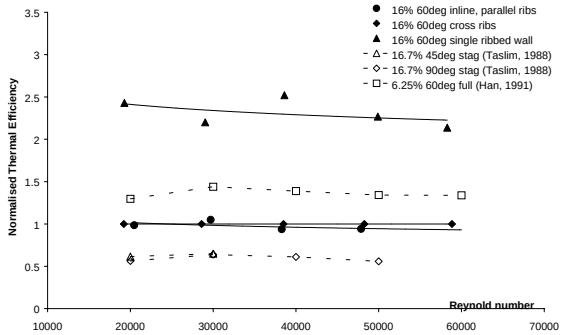

Figure 16 Comparison of the normalized thermal efficiency of the ribbed wall between different configurations

Conclusion

Three 16% blockage 60^{o}, interrupted ribs configurations were tested for heat transfer and pressure loss performance and the results were compared with data in the literature for similar blockage and rib inclinations. The following conclusions can be drawn.

1) 16% blockage ribs system do not have significantly higher heat transfer than the 6% blockage ribs system, Webb (1994) pointed out that ribs with blockage ratios higher than 8% do not improve heat transfer. However, in situations where roughness elments are inevitably large due to casting limitation, these data will be useful to turbine blade designers.
2) Apart from distrupting the boundary layer, the ribs also enhance heat transfer by favorable secondary flow.
3) The structure of the induced secondary flow is determined by the ribs incidence and the ribs orientation on the facing wall. Two counter rotating vortices were induced by the in-line, parallel ribs and a single vortex is induced by the cross ribs and single ribbed wall configuration.
4) Two counter rotating vortices enhance the flow mixing in the passage, and the hot core flow is disturbed which results the in-line, parallel rib configuration achieving the highest heat transfer for the configurations tested.
5) The single vortex in the single ribbed wall configuration takes at least 7 rib rows in order to be established. This causes this configuration to achieve the lowest htc of the configurations tested. Because of its small friction loss, this configuration achieved the best thermal efficiency on the ribbed wall heat transfer for the configuration studied.
6) Heat transfer enhancement decrease as Reynolds number increases, this could imply the favorable secondary flow effect reduces as the axial flow velocity increases.

Acknowledgements

This work has been carried out with the support of Rolls-Royce Plc. and the DERA, MOD and DTI, the continuance of which is greatly appreciated, as is their permission to publish this work. The lead author was supported at Oxford University by the Croucher Foundation. The technical assistance of Mr. P.J. Timms was also much appreciated.

Nomenclature

A	Area, m^2
Cp	specific heat, J/kgK
d, D	passage hydraulic diameter, m
e	rib height, m
f	friction factor, Eqn. 1
h, htc	heat transfer coefficient, Wm^2K
k	thermal conductivity of air, W/mK
m	mass flow, kg/s
Nu	Nusselt Number, Nu=hD/k
p	pitch length, m
P	Pressure, Pa
Re	Reynolds number, Ud/ν
U	main stream flow velocity, m/s
x	length in streamwise direction, m

Greek	fluid density, kg/m^3
ρ	viscosity, Ns/m^2
ν	

Subscript	
avg	average
cl	centre-line
e	overall ribs
mb	mixed bulk
s	smooth wall
total	total rib suface
us	upstream

References

Carslaw, H.S. and Jaeger, J.C., 1959. “Conduction of heat in solids”, Clarendon Press, Oxford, pp.334-339

Fann, S., Yang, W.J., Zhang, N., 1994, “Local heat transfer in a rotating serpentine passage with rib-roughened surfaces”, Journal of heat and mass transfer, Vol. 37, No.2, pp.217-228.

Gillespie, D.R.H., 1996, DPhil thesis, Department of Engineering Science, University of Oxford.

Han, J.C., Zhang, Y.M., Lee, C.P., 1991. “Augmented heat transfer in square channels with parallel, crossed, and V-shaped angled ribs”, Journal of Turbomachinery, Vol. 113, pp.590-596

Ireland, P.T., Tsang, C.L.P., Dailey, G.M., 2001. “Reduced instrumentation testing of blade cooling passages”, NATO, RTA/AVT, Norway, May 2001.

Kukreja, R.T., Lau, S.C., McMillin, R.D., 1992. “Effects of length and configuration of transverse discrete ribs on heat transfer and friction for turbulent flow in a square channel”, International Journal of Turbo and Jet Engines, vol. 9, pp.301-310.

Main, A.J., Day, C.R.B., Lock, G.D., Oldfield, M.L.G., 1996. “Calibration of a four-hole pyramid probe and area traverse measurements in a short-duration transonic turbine cascade tunnel”, Experiments in Fluids, vol. 21, pp.302-311.

Metzger D.E. and Larson, D.E. 1986, “Use of melting point surface coatings for local convection heat transfer measurements in rectangular channel flows with 90-deg turns”, J. Heat Transfer, vol.108, pp.48-54.

Rau, G., Cakan, M., Moeller, D., Arts, T., “The effect of periodic ribs on the local aerodynamic and heat transfer performance of a straight cooling channel”, Journal of Turbomachinery, vol.120, pp.368-375.

Taslim, M.E. and Spring S.D., 1988, “Experimental study of heat transfer and friction factors in turbulated cooling passages of different aspect ratios, where turbulators are staggered”, AIAA-88-3014.

Taslim, M.E.,, Li, T. and Kercher, D.M., 1996, “Experimental heat transfer and friction in channels roughened with angled, V-shaped, and discrete ribs on two opposite walls”, Journal of Turbomachinery, Vol. 118, pp.1-9.

Tsang, C.L.P., Gillespie, D.R.H., Ireland, P.T., Dailey, G.M., 2000. “Analysis of transient heat transfer experiments”, Proceedings of the 8th International Symposium on Transport Phenomena and Dynamics of Rotating Machinery. pp. 714-721.

Wang, Z., Ireland P.T., Kohler, S.T. and Chew J.W., 1996. “Heat transfer measurements to a gas turbine cooling passage with inclined ribs”, J. of Turbomachinery, Vol. 120, pp.63-69.

Webb, R.L., 1994. “Principles of enhanced heat transfer”, John Wiley and Sons, chapter 9.

Paper Number: 18

Name of Discusser: T. Arts, Von Karman Institute Rhode Saint Genese, Belgium

Question:
Could you comment on the relative contributions along the different walls, including the ribs, of the heat transfer for the configurations tested in this investigation?

Answer:
The respective contribution of the different heat transfer surfaces can be found by averaging the local data in figures 7 – 9. In each case the level is expressed with respect to the contribution of the ribbed wall in the 16 %, 60 degree interrupted parallel rib configuration. Note that in the case of the single ribbed wall configuration the overall heat transfer is lower so the additional smooth wall has an average normalised htc of 0.2 – 0.3.

surface Config.	Top	Ribbed	Bottom
Parallel 16 % 60 % int.	0,51	1	0,67
Crossed 16 % 60 % Int.	0,54	0,92	0,58
Single Wall 16 % 60 % Int.	0,4	1	0,67

Table: Normalised average area weighted heat transfer coefficient.

Name of Discusser: H. Weyer, DLR Cologne

Question:
1 Are the ribs realistic in terms of a turbine cooling channel?
2 Blade rotation will affect and alter secondary flow. Can the stationary data be transferred to the rotating system?

Answer:
1 Yes, while large ribs may not necessarily be desirable, the incorporation of small cast passages into the blade wall, see papers 25 and 26, means that the minimum manufacturable turbulator size will rise to 15 – 30 % of the passage height.

2 The very strong secondary flows induced by the ribs are likely to persist in the rotating case, although they will interact with rotation effects. Stationary tests provide a cost effective means to assess many possible geometries, and to select the best available technology. Further testing in a rotating environment would, of course, be desirable.